Energy levels in a symmetric triple well

Author: Ferran Torra Clotet
*Facultat de Física, Universitat de Barcelona, Diagonal 645, 08028 Barcelona, Spain.**

Advisor: Josep Taron

Abstract: We show, by analogy with the double square well, the energy levels of the triple square well. More specifically, it is interesting the analysis of the lowest energy levels when $E < V_0$ because the three lowest energy levels are non-degenerate in contrast with the classical solution, and the transition between different wells is possible. As a result, we develop the corresponding energy formulae which are confirmed numerically and the tunnel effect is also described.

I. INTRODUCTION

Classically, in a symmetric double well, for $E < V_0$, there are two ground states of equal energy. In contrast, the quantum solution provides a splitting of the two lowest energy levels and the probabilities of the corresponding wave functions are nonzero in classically forbidden regions. In particular, it is shown in [2] with a square well potential.

As an extension of the results presented in [2], we are going to develop the triple square well case and the tunnelling processes involved in this potential. In addition, we will verify properties that hold for all one dimensional symmetric potentials (see [3]):

- bound energy levels in one-dimensional potentials are non-degenerate,
- the wave function of the ground state is symmetric and the eigenstates are alternately symmetric and antisymmetric with respect to the centre of symmetry, $x = 0$.

This document, initially, provides an analysis of the two types of possible solutions of the one-dimensional Schrödinger equation in a symmetric potential and then we determine the corresponding energy levels. These results are compared with the numerical calculations in order to validate our approximations. Finally, the tunnel effect is discussed with the consideration of interesting wave functions.

We consider the symmetric triple well potential (represented in Fig. 1) of the form,

$$V(x) = \begin{cases} \infty, & |x| > 3\frac{L}{2} + w, \\ 0, & \text{regions } I, III, V, \\ V_0, & \text{regions } II, IV, \end{cases} \tag{1}$$

where L is the width of a single square well, w is the width of the potential barrier and V_0 is the barrier height.

Our interest is in the case $E < V_0 \to \infty$ where classically there are three ground energy levels corresponding to the movement of a particle in each single well. The quantum possibility of a particle to tunnel through the barriers produces a splitting of these levels into three non-degenerate energy levels.

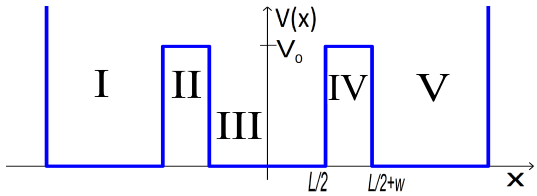

Figure 1: The triple square well potential.

In addition, observe that there are two semi-infinite square wells and one finite square well. This fact will be relevant for the structure of the energy levels as it is going to be demonstrated in this work.

II. WAVE FUNCTIONS

Since the potential is symmetric with respect to the origin, the solutions of the time-independent Schrödinger equation will be wave functions of definite parity. In addition, we have to take into account the boundary conditions, $\psi(-\frac{3}{2}L - w) = \psi(\frac{3}{2}L + w) = 0$. Therefore, the eigenfunctions of the Hamiltonian for $E < V_0$ can be written as one of the following forms,

- symmetric solutions,

$$\psi(x) = \begin{cases} D\sin[k(w + \frac{3}{2}L + x)] & I, \\ B\sinh[\alpha(\frac{w}{2} + \frac{L}{2} + x)] + \\ \quad + C\cosh[\alpha(\frac{w}{2} + \frac{L}{2} + x)] & II, \\ A\cos kx & III, \\ B\sinh[\alpha(\frac{w}{2} + \frac{L}{2} - x)] + \\ \quad + C\cosh[\alpha(\frac{w}{2} + \frac{L}{2} - x)] & IV, \\ D\sin[k(w + \frac{3}{2}L - x)] & V, \end{cases} \tag{2}$$

*Electronic address: ftorracl9@alumnes.ub.edu

- antisymmetric solutions

$$\psi(x)=\begin{cases} -D\sin[k(w+\frac{3}{2}L+x)] & I, \\ \begin{array}{l}-B\sinh[\alpha(\frac{w}{2}+\frac{L}{2}+x)]- \\ -C\cosh[\alpha(\frac{w}{2}+\frac{L}{2}+x)]\end{array} & II, \\ A\sin kx & III, \\ \begin{array}{l}B\sinh[\alpha(\frac{w}{2}+\frac{L}{2}-x)]+ \\ +C\cosh[\alpha(\frac{w}{2}+\frac{L}{2}-x)]\end{array} & IV, \\ D\sin[k(w+\frac{3}{2}L-x)] & V, \end{cases} \quad (3)$$

where $k=\frac{\sqrt{2mE}}{\hbar}$ and $\alpha=\frac{\sqrt{2m(V_0-E)}}{\hbar}$.

In both cases, the solutions must satisfy the continuity conditions for the wave function and its derivative at the points $x=\pm\frac{L}{2}$ and $x=\pm(\frac{L}{2}+w)$. Note that, since the eigenfunctions have definite parity, it suffices to analyze the conditions at the points $x=\frac{L}{2}$ and $x=\frac{L}{2}+w$.

A. Symmetric solutions

On the one hand, the conditions at the point $x=\frac{L}{2}$ in matricial form are,

$$A\begin{pmatrix}\cos k\frac{L}{2} \\ -k\sin k\frac{L}{2}\end{pmatrix}=\begin{pmatrix}\sinh\frac{\alpha w}{2} & \cosh\frac{\alpha w}{2} \\ -\alpha\cosh\frac{\alpha w}{2} & -\alpha\sinh\frac{\alpha w}{2}\end{pmatrix}\begin{pmatrix}B \\ C\end{pmatrix}. \quad (4)$$

Inverting the matrix, we can isolate the terms B and C,

$$\begin{pmatrix}B \\ C\end{pmatrix}=A\begin{pmatrix}-\sinh\frac{\alpha w}{2} & -\frac{1}{\alpha}\cosh\frac{\alpha w}{2} \\ \cosh\frac{\alpha w}{2} & \frac{1}{\alpha}\sinh\frac{\alpha w}{2}\end{pmatrix}\begin{pmatrix}\cos k\frac{L}{2} \\ -k\sin k\frac{L}{2}\end{pmatrix}. \quad (5)$$

On the other hand, the conditions at the point $x=\frac{L}{2}+w$ in matricial form are,

$$D\begin{pmatrix}\sin kL \\ -k\cos kL\end{pmatrix}=\begin{pmatrix}-\sinh\frac{\alpha w}{2} & \cosh\frac{\alpha w}{2} \\ -\alpha\cosh\frac{\alpha w}{2} & \alpha\sinh\frac{\alpha w}{2}\end{pmatrix}\begin{pmatrix}B \\ C\end{pmatrix}. \quad (6)$$

Thus, using (5), we get the following relationship,

$$D\begin{pmatrix}\sin kL \\ -k\cos kL\end{pmatrix}=A\begin{pmatrix}\cosh\alpha w & \frac{1}{\alpha}\sinh\alpha w \\ \alpha\sinh\alpha w & \cosh\alpha w\end{pmatrix}\begin{pmatrix}\cos k\frac{L}{2} \\ -k\sin k\frac{L}{2}\end{pmatrix}. \quad (7)$$

Dividing the two rows of (7), it leads to the condition

$$\tan kL = -\frac{k}{\alpha}\left[\frac{\cot\left(k\frac{L}{2}\right)-\frac{k}{\alpha}\tanh(\alpha w)}{\tanh(\alpha w)\cot\left(k\frac{L}{2}\right)-\frac{k}{\alpha}}\right]. \quad (8)$$

This expression can also be written as

$$\frac{2\zeta}{\zeta^2-1}=-\epsilon\frac{\zeta-\epsilon\eta}{\eta\zeta-\epsilon}, \quad (9)$$

where $\zeta\equiv\cot\left(k\frac{L}{2}\right)$, $\epsilon\equiv\frac{k}{\alpha}$ and $\eta\equiv\tanh(\alpha w)$. And finally,

$$\epsilon\zeta^3+(2-\epsilon^2)\eta\zeta^2-3\epsilon\zeta+\epsilon^2\eta=0. \quad (10)$$

Observe that, when $\epsilon=0$, this equation becomes $2\eta\zeta^2=0$ which has only one root $\zeta=0$ (of multiplicity 2) because $\eta\neq 0$. Thus, there are two roots of the perturbed equation near $\zeta_0=0$. Assuming the expansion $\zeta(\epsilon)=\zeta_0+\zeta_1\epsilon+\zeta_2\epsilon^2+\ldots$, we get the solutions,

$$\zeta=\left[3\pm\sqrt{9-8\eta^2}\right]\frac{\epsilon}{4\eta}+o(\epsilon^2). \quad (11)$$

Recovering the original notation, this condition is

$$\cot\frac{kL}{2}\simeq\frac{k}{\alpha}\frac{1}{4\tanh\alpha w}\left[3\pm\sqrt{9-8\tanh^2(\alpha w)}\right]. \quad (12)$$

B. Antisymmetric solutions

The conditions at $x=\frac{L}{2}$ in matricial form are,

$$A\begin{pmatrix}\sin k\frac{L}{2} \\ k\cos k\frac{L}{2}\end{pmatrix}=\begin{pmatrix}\sinh\frac{\alpha w}{2} & \cosh\frac{\alpha w}{2} \\ -\alpha\cosh\frac{\alpha w}{2} & -\alpha\sinh\frac{\alpha w}{2}\end{pmatrix}\begin{pmatrix}B \\ C\end{pmatrix}. \quad (13)$$

Inverting the matrix, we can isolate the terms B and C,

$$\begin{pmatrix}B \\ C\end{pmatrix}=A\begin{pmatrix}-\sinh\frac{\alpha w}{2} & -\frac{1}{\alpha}\cosh\frac{\alpha w}{2} \\ \cosh\frac{\alpha w}{2} & \frac{1}{\alpha}\sinh\frac{\alpha w}{2}\end{pmatrix}\begin{pmatrix}\sin k\frac{L}{2} \\ k\cos k\frac{L}{2}\end{pmatrix}. \quad (14)$$

The conditions at $x=\frac{L}{2}+w$ in matricial form are,

$$D\begin{pmatrix}\sin kL \\ -k\cos kL\end{pmatrix}=\begin{pmatrix}-\sinh\frac{\alpha w}{2} & \cosh\frac{\alpha w}{2} \\ -\alpha\cosh\frac{\alpha w}{2} & \alpha\sinh\frac{\alpha w}{2}\end{pmatrix}\begin{pmatrix}B \\ C\end{pmatrix}. \quad (15)$$

Thus, using (14), we get the following relationship,

$$D\begin{pmatrix}\sin kL \\ -k\cos kL\end{pmatrix}=A\begin{pmatrix}\cosh\alpha w & \frac{1}{\alpha}\sinh\alpha w \\ \alpha\sinh\alpha w & \cosh\alpha w\end{pmatrix}\begin{pmatrix}\sin k\frac{L}{2} \\ k\cos k\frac{L}{2}\end{pmatrix}. \quad (16)$$

Dividing the two rows of (16), it leads to the condition

$$\tan kL = -\frac{k}{\alpha}\left[\frac{1+\frac{k}{\alpha}\tanh(\alpha w)\cot\left(k\frac{L}{2}\right)}{\tanh(\alpha w)+\frac{k}{\alpha}\cot\left(k\frac{L}{2}\right)}\right]. \quad (17)$$

This expression can also be written as

$$\frac{2\zeta}{\zeta^2-1}=-\epsilon\frac{1+\epsilon\eta\zeta}{\eta+\epsilon\zeta}, \quad (18)$$

where $\zeta\equiv\cot\left(k\frac{L}{2}\right)$, $\epsilon\equiv\frac{k}{\alpha}$ and $\eta\equiv\tanh(\alpha w)$. And finally,

$$\epsilon^2\eta\zeta^3+3\epsilon\zeta^2+(2-\epsilon^2)\eta\zeta-\epsilon=0. \quad (19)$$

Note that, when $\epsilon=0$, this equation becomes $2\eta\zeta=0$ which has only one root $\zeta=0$ (of multiplicity 1) because $\eta\neq 0$. Thus, there is one root of the perturbed equation near $\zeta_0=0$. Assuming the expansion $\zeta(\epsilon)=\zeta_0+\zeta_1\epsilon+\zeta_2\epsilon^2+\ldots$, we get the solution,

$$\zeta=\frac{\epsilon}{2\eta}+o(\epsilon^2). \quad (20)$$

Recovering the original notation, this condition is

$$\cot\frac{kL}{2}\simeq\frac{k}{\alpha}\frac{1}{2\tanh\alpha w}. \quad (21)$$

III. ENERGY LEVELS

Let k_G, k_F and k_S be the three lowest values of k corresponding to the ground state (ψ_G), the first excited state (ψ_F) and the second excited state (ψ_S).

These three quantities are obtained from (12) and (21) and they are located around $kL \sim \pi$. Our assumption is to consider the case where the height V_0 of the potential barrier is huge compared with the minimum energy level E, therefore $\alpha \sim \frac{\sqrt{2mV_0}}{\hbar} = \alpha_0 \gg k$. Moreover, we consider that the width of the barrier is such that $\alpha_0 w \gg 1$.

Consequently, these three values appear as the intersections of $y = \cot\frac{kL}{2}$ with the straight lines $y = \varepsilon_G \frac{kL}{2}$, $y = \varepsilon_F \frac{kL}{2}$ and $y = \varepsilon_S \frac{kL}{2}$ near $kL \sim \pi$, where the constants are

$$\varepsilon_G = \frac{\coth(\alpha_0 w)}{\alpha_0 L}\left[\frac{3+\sqrt{9-8\tanh^2(\alpha_0 w)}}{2}\right], \quad (22)$$

$$\varepsilon_F = \frac{\coth(\alpha_0 w)}{\alpha_0 L}, \quad (23)$$

$$\varepsilon_S = \frac{\coth(\alpha_0 w)}{\alpha_0 L}\left[\frac{3-\sqrt{9-8\tanh^2(\alpha_0 w)}}{2}\right]. \quad (24)$$

Thus, since $k \sim \pi/L$, we find the following approximate values,

$$k_G \simeq \frac{\pi}{L(1+\varepsilon_G)}, \quad k_F \simeq \frac{\pi}{L(1+\varepsilon_F)}, \quad k_S \simeq \frac{\pi}{L(1+\varepsilon_S)}. \quad (25)$$

Note that, in our range of parameters, the three constants satisfy $\varepsilon_S < \varepsilon_F < \varepsilon_G \ll 1$. Hence, the three quantities are slightly smaller than π/L which corresponds to the lowest value of the wave number in an individual infinite well of width L. In addition, these three quantities satisfy $k_G < k_F < k_S$ and the respective energies are

$$E_G = \frac{\hbar^2 k_G^2}{2m}, \quad E_F = \frac{\hbar^2 k_F^2}{2m}, \quad E_S = \frac{\hbar^2 k_S^2}{2m}, \quad (26)$$

where E_G is the ground state energy, E_F is the first excited state energy and E_S is the second excited state energy such that $E_G < E_F < E_S$.

Observe that the wave functions of the ground state and the second excited state are symmetric, and the wave function of the first excited state is antisymmetric, as we expected.

We notice that the conditions of (12) and (21) are valid for any group of energy levels of *odd* order (i.e. with kL in the vicinity of a odd multiple of π) because the assumption was that $\cot\left(k\frac{L}{2}\right) = 0$, which is valid for $k\frac{L}{2} = (2n+1)\pi$ with $n \in \mathbb{Z}$. Therefore, the $(6n)^{th}$ excited state and the $(6n+2)^{th}$ excited state are symmetric and the $(6n+1)^{th}$ excited state is antisymmetric for all $n \in \mathbb{N}$.

Moreover, for any group of energy levels of *even* order (i.e. with kL in the vicinity of a even multiple of π), we should analyze the solutions from (8) and (17) around $\zeta' = \tan\left(k\frac{L}{2}\right)$, which leads to the following respective equations,

$$\epsilon^2\eta(\zeta')^3 - 3\eta(\zeta')^2 + (2-\epsilon^2)\eta\zeta' + \epsilon = 0, \quad (27)$$

$$-\epsilon(\zeta')^3 + (2-\epsilon^2)\eta(\zeta')^2 + 3\epsilon\zeta' + \epsilon^2\eta = 0. \quad (28)$$

In a similar way as in (19), the symmetric case has only one solution located in the vicinity of $kL \sim 2n\pi$ for all $n \in \mathbb{N}$. Likewise, the antisymmetric case has two solutions around each $kL \sim 2n\pi$ for all $n \in \mathbb{N}$. Thus, the $(3(2n+1))^{th}$ excited state and the $(3(2n+1)+2)^{th}$ excited state are antisymmetric and the $(3(2n+1)+1)^{th}$ excited state is symmetric for all $n \in \mathbb{N}$.

With this point of view, the energy levels are non-degenerate as expected since we are dealing with states of one-dimensional potential. Moreover, it is interesting to note that the energy spectrum consists of alternating symmetric and antisymmetric states where the ground state is always symmetric, the first excited state is antisymmetric, and so on.

Furthermore, it is interesting to analyze the gap between these energy levels.

On the one hand, between the ground state and the first excited state, it is given by,

$$E_F - E_G \simeq \frac{\hbar^2\pi^2}{2mL^2}\left[\frac{1}{(1+\varepsilon_F)^2} - \frac{1}{(1+\varepsilon_G)^2}\right] \simeq \quad (29)$$

$$\simeq \frac{\hbar^2\pi^2}{mL^2}(\varepsilon_G - \varepsilon_F) = \quad (30)$$

$$= \frac{\hbar^2\pi^2}{mL^2}\frac{\coth(\alpha_0 w)}{\alpha_0 L}\left[\frac{1}{2} + \frac{\sqrt{9-8\tanh^2(\alpha_0 w)}}{2}\right]. \quad (31)$$

According to the assumption that $\alpha_0 w \gg 1$, we have $\coth(\alpha_0 w) \simeq 1 + 2e^{-2\alpha_0 w}$ and $\tanh(\alpha_0 w) \simeq 1 - 2e^{-2\alpha_0 w}$. Therefore,

$$E_F - E_G \simeq \frac{\hbar^2\pi^2}{mL^2}\frac{(1+2e^{-2\alpha_0 w})(1+8e^{-2\alpha_0 w})}{\alpha_0 L} \simeq \quad (32)$$

$$\simeq \frac{\hbar^2\pi^2}{mL^2}\frac{1}{\alpha_0 L}. \quad (33)$$

We see that this gap decreases as $1/\alpha_0$ when α_0 (i.e. the height of the potential barrier, V_0) increases.

On the other hand, the split between the first excited state and the second one is

$$E_S - E_F \simeq \frac{\hbar^2\pi^2}{2mL^2}\left[\frac{1}{(1+\varepsilon_S)^2} - \frac{1}{(1+\varepsilon_F)^2}\right] \simeq \quad (34)$$

$$\simeq \frac{\hbar^2\pi^2}{mL^2}(\varepsilon_F - \varepsilon_S) = \quad (35)$$

$$= \frac{\hbar^2\pi^2}{mL^2}\frac{\coth(\alpha_0 w)}{\alpha_0 L}\left[-\frac{1}{2} + \frac{\sqrt{9-8\tanh^2(\alpha_0 w)}}{2}\right]. \quad (36)$$

Applying the same assumption used in the other gap,

$$E_S - E_F \simeq \frac{\hbar^2\pi^2}{mL^2}\frac{(1+2e^{-2\alpha_0 w})(8e^{-2\alpha_0 w})}{\alpha_0 L} \simeq \quad (37)$$

$$\simeq \frac{\hbar^2\pi^2}{mL^2}\frac{8e^{-2\alpha_0 w}}{\alpha_0 L}. \quad (38)$$

Note that, in this case, the gap decreases exponentially when α_0 (i.e. the height of the potential barrier, V_0) increases.

Thus, the ground state and the first excited state are more separated than the first and the second excited states.

IV. NUMERICAL SOLUTION

To verify our equations, we solve (8) and (17) with numerical methods using [4]. We show the results of the values of k corresponding to the three eigenstates of lowest energy. In this section, the unit of distance will be L and, consequently, the unit of wave number k and α_0 will be L^{-1}.

We present Table I, where the assumptions mentioned above are clearly satisfied. Therefore, our results are consistent with the numerical solutions.

$\alpha_0[L^{-1}]$	100	300	500
$k_G[L^{-1}]$	3.07381	3.1207869	3.12907627
$k_G^{num}[L^{-1}]$	3.07563	3.1207863	3.12907635
$k_F[L^{-1}]$	3.10933	3.1311553	3.1353219685
$k_F^{num}[L^{-1}]$	3.10934	3.1311551	3.13532200954
$k_S[L^{-1}]$	3.11335	3.1311556	3.1353219686
$k_S^{num}[L^{-1}]$	3.11149	3.1311557	3.13532200959

Table I: The numerically calculated quantities of k corresponding to the lowest three energy levels against those predicted using our equations for $w = 0.02L$ and different values of α_0.

The results with a small height of the potential barrier (Table II) are also consistent with what we might predict based on equations above.

$w[L]$	0.2	0.35	0.5
$k_G[L^{-1}]$	2.58683	2.61640	2.61791
$k_G^{num}[L^{-1}]$	2.56951	2.61025	2.61273
$k_F[L^{-1}]$	2.84634	2.85552	2.85597
$k_F^{num}[L^{-1}]$	2.84243	2.85179	2.85231
$k_S[L^{-1}]$	2.86448	2.85646	2.85602
$k_S^{num}[L^{-1}]$	2.87891	2.85408	2.85244

Table II: The numerically calculated quantities of k corresponding to the lowest three energy levels against those predicted using our equations for $\alpha_0 = 10/L$ and different values of w .

Note that these three energy levels are not equidistant, as we expected due to the central well is different of the other ones.

Furthermore, we can obtain the parameters of symmetric solutions (2) (resp. antisymmetric solutions (3)) by solving numerically (4) and (5) (resp. (13) and (14)); and, of course, using the normalization condition. These coefficients are given in Table III for the lowest three energy levels with $w = 0.02L$ and $\alpha_0 = 100/L$.

	A	B	C	D
ψ_G	1.327	$1.01\cdot10^{-2}$	$2.14\cdot10^{-2}$	$3.13\cdot10^{-1}$
ψ_F	$8.52\cdot10^{-3}$	$-1.00\cdot10^{-2}$	$1.32\cdot10^{-2}$	$9.95\cdot10^{-1}$
ψ_S	$4.46\cdot10^{-1}$	$1.40\cdot10^{-2}$	$-6.60\cdot10^{-3}$	$-9.44\cdot10^{-1}$

Table III: Coefficients of the eigenstates ψ_G, ψ_F and ψ_S of the Hamiltonian with $w = 0.02L$ and $\alpha_0 = 100/L$.

These wave functions can be represented graphically (Fig. 2).

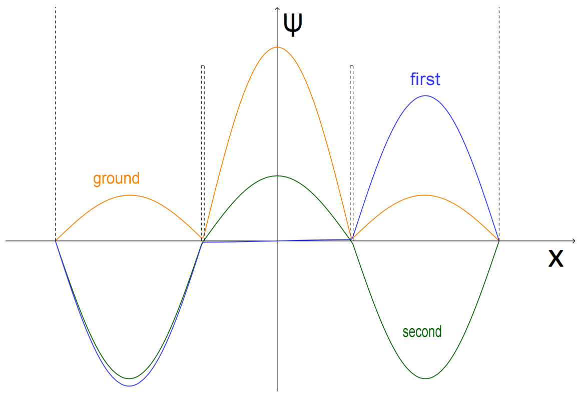

Figure 2: Wave functions for the lowest three energy levels with $w = 0.02L$ and $\alpha_0 = 100/L$. Orange line corresponds to the ground state (ψ_G), blue line to the first excited state (ψ_F) and green line to the second excited state (ψ_S).

V. THE TUNNEL EFFECT

Classically, in our configuration, there are three ground states of equal energy, one for each single square well. However, the three lowest energy quantum levels are nondegenerate and the probability density of these eigenstates in the regions II and IV is nonzero, whereas these regions are classically forbidden.

We can combine the wave functions to get the following configurations

$$\psi_C(x) = \frac{1}{N_C}(-D_S\psi_G(x) + D_G\psi_S(x)), \quad (39)$$

where $N_C = \sqrt{D_G^2 + D_S^2}$, and

$$\psi_L(x) = \frac{1}{N_L}\left(A_S^2\psi_G(x) - A_G^2\psi_S(x) + \right. \tag{40}$$

$$\left. + \frac{(A_G D_S - A_S D_G)}{D_F}\psi_F(x)\right), \tag{41}$$

$$\psi_R(x) = \frac{1}{N_L}\left(A_S^2\psi_G(x) - A_G^2\psi_S(x) - \right. \tag{42}$$

$$\left. - \frac{(A_G D_S - A_S D_G)}{D_F}\psi_F(x)\right), \tag{43}$$

where $N_L = \sqrt{A_G^2 + A_S^2 + \frac{(A_G D_S - A_S D_G)^2}{D_F^2}}$.

These configurations can be interpreted as the classical configurations because they are practically localised in a single square well as shown in Fig. 3.

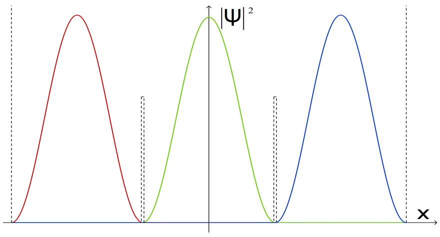

Figure 3: Probability densities of the classical configurations with the parameters $w = 0.02L$ and $\alpha_0 = 100/L$; red line corresponds to ψ_L, green line to ψ_C and blue line to ψ_R.

More interesting is to consider a wave function $\psi_1(x,t)$ which initially is equal to ψ_C, i.e., located in the central square well. Its time evolution can be expressed,

$$\psi_1(x,t) = \frac{1}{N_C}\left(D_G\psi_S(x)e^{-i\frac{E_S t}{\hbar}} - D_S\psi_G(x)e^{-i\frac{E_G t}{\hbar}}\right) = \tag{44}$$

$$= \frac{e^{-i\frac{E_G t}{\hbar}}}{N_C}\left(-D_S\psi_G(x) + D_G\psi_S(x)e^{-i\omega t}\right), \tag{45}$$

where $\hbar\omega = E_S - E_G$.

Observe that the probability density varies periodically with the frequency ω. Indeed, the particle can be displaced to the other square wells (with major probability after a time $t = \pi/\omega$) because of quantum tunnelling (see Fig. 4) and then it is turned back to the center square well .

Moreover, the same idea can be applied for a wave function $\psi_2(x,t)$ located at the left square well at $t = 0$. This wave function can describe a time evolution which permits a major probability density in the right configuration because the quantum tunnelling again. Unfortunately, this evolution cannot be expressed with a exact frequency because there are two exponentials terms,

$$\psi_2(x,t) = \frac{1}{N_L}\left(A_S^2\psi_G(x)e^{-i\frac{E_G t}{\hbar}} - A_G^2\psi_S(x)e^{-i\frac{E_S t}{\hbar}} + \right. \tag{46}$$

$$\left. + \frac{(A_G D_S - A_S D_G)}{D_F}\psi_F(x)e^{-i\frac{E_F t}{\hbar}}\right) = \tag{47}$$

$$= \frac{e^{-i\frac{E_G t}{\hbar}}}{N_L}\left(A_S^2\psi_G(x) - A_G^2\psi_S(x)e^{-i\omega_S t} + \right. \tag{48}$$

$$\left. + \frac{(A_G D_S - A_S D_G)}{D_F}\psi_F(x)e^{-i\omega_F t}\right), \tag{49}$$

where $\hbar\omega_F = E_F - E_G$ and $\hbar\omega_S = E_S - E_G$.

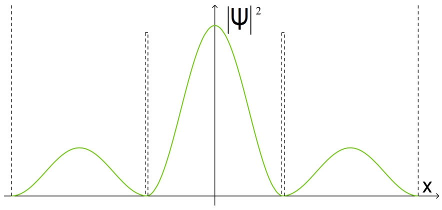

Figure 4: Probability density of $\psi_1(x,t)$ after a time $t = \pi/\omega$.

VI. CONCLUSIONS

In this essay, we have shown that the three lowest energy levels are non-degenerate but they are not equidistant. Our formulae have been confirmed with numerical calculations and they show an example of the quantum tunnelling phenomena.

Our results are consistent with the symmetric triple well using instanton methods which is explained in [1].

As a final comment, we expect that the N lowest energy levels in N square wells are non-degenerate and they tend to create an energy band.

Acknowledgments

I would like to thank my advisor Josep Taron for all useful discussions and corrections. I would also like to thank the support received from my friends and family, especially my parents.

[1] H. A. Alhendi and E. I. Lashin, Mod.Phys.Lett. **A19**, 2103-2112 (2004).
[2] J. L. Basdevant and J. Dalibard, *Quantum mechanics*, 2nd. ed. (Springer, Berlin, 2006).
[3] A. Messiah, *Quantum mechanics*, Vol. 1 (North-Holland, Amsterdam, 1961).
[4] Wolfram Research, Inc., *Mathematica*, Version 10.4 (Champaign, 2016).